A Characterization Study Relating Cross-Sectional Distribution of Fiber Volume Fraction and Permeability

Rasmussen, Filip S.; Sonne, Mads R.; Larsen, Martin ; Mikkelsen, Lars P.; Hattel, Jesper H.

Published in:
Proceedings of 22nd International Conference on Composite Materials

Publication date:
2019

Document Version
Publisher's PDF, also known as Version of record

A CHARACTERIZATION STUDY RELATING CROSS-SECTIONAL DISTRIBUTION OF FIBER VOLUME FRACTION AND PERMEABILITY

Filip S. Rasmussen[1*], Mads R. Sonne[1], Martin Larsen[2], Lars P. Mikkelsen[3] and Jesper H. Hattel[1]

[1] Department of Mechanical Engineering, Technical University of Denmark (DTU), 2800 Kgs. Lyngby, Denmark.
[2] Fiberline Composites A/S, 550 Middelfart, Denmark.
[3] Department of Wind Energy, DTU, 4000 Roskilde, Denmark.
* Corresponding author: fsras@mek.dtu.dk

Keywords: Fiber Distribution, Permeability, Scanning Electron Microscopy, Impregnation.

ABSTRACT

In the present study, Scanning Electron Microscopy (SEM) has been used to assess the influence of a varying cross-sectional fiber volume fraction on local permeability values. The investigated sample is a textured glass fiber reinforced polyurethane composite rod with an Ø5mm cross-section. The SEM investigations show a high variation in local fiber volume fraction with a mean fiber volume fraction of 0.41±0.2, which is in agreement with the value 0.41 obtained by burn-off test by the manufacturer. The additional result from the SEM investigations was a mean fiber diameter of 23.2±2.6µm, which was verified by single fiber tests. The characterization results were successfully used to evaluate the local variation in permeability over the cross-section and could most likely be a very essential input for numerical impregnation simulations.

1 INTRODUCTION

Composite materials, in the form of Fiber Reinforced Polymers (FRP), are often manufactured using resin transfer processes, e.g. Vacuum Assisted Resin Transfer Moulding (VARTM) or Resin Injection Pultrusion (RIP). The final quality of the FRPs are known to be influenced by the design of the impregnation process, i.e. ensuring complete wet-out, hence minimizing void formation. When designing the impregnation process one of the key parameters is the permeability of the fibrous pre-form [1]. The permeability is often assumed to obey the Kozeny-Carman equation

$$K = \frac{R^2}{4k}\frac{(1-V_f)^3}{{V_f}^2} \tag{1}$$

where k is the Kozeny constant, V_f the fiber volume fraction and R the fiber radius. The Kozeny-Carman equation (1) was originally derived for granular beds [2] but has since also been assumed valid for porous fiber beds consisting of continuous unidirectional (UD) fibers. A modification of (1), including that the transverse flow will stop when the maximum fiber volume fraction is reached, was proposed by Gebart [3]

$$K_{\perp} = \frac{8R^2}{c}\frac{(1-V_f)^3}{{V_f}^2} \tag{2}$$

$$K_{||} = C_1\left(\sqrt{\frac{V_{f\,max}}{V_f}} - 1\right)^{5/2} R^2 \tag{3}$$

In (2) and (3) the constants C_1 and c are fiber packing factors assuming either quadratic or hexagonal fiber packing.

In the work by Bechtold [4] a representative volume containing 15 fibers was investigated using a numerical approach. The position of the 15 fibers was then changed and the resulting transverse permeability simulated. The results showed that the permeability is not only a function of fiber volume fraction but also a function of the relative fiber position, i.e. degree of fiber agglomeration. An experimental investigation of permeability and capillary pressure conducted by Ahn and Seferis for woven fabrics [5], concluded that the Kozeny-Carman equation was adequate for fiber volume fractions up to 0.5. An experimental investigation by Bezerra et al. includes permeability characterization of fiber rovings [6]. The results for longitudinal permeability showed good agreement with literature while the characterized transverse permeability was lower than expected.

The objective of the present study is to characterize the cross-section of a textured glass fiber polyurethane (GF-PUR) rod with a diameter of 5mm using Scanning Electron Microscopy (SEM). The rod is a turned down centre part from a larger composite beam. The micrographs from SEM are analysed using MATLAB to obtain the cross-sectional distribution of fiber volume fraction as well as fiber diameter distribution. The results obtained by SEM are verified by two supplementary studies; 1) Light Optical Microscopy (LOM) including stitching of the micrographs to obtain an overview image of the full Ø5mm cross-section, and 2) Single Fiber Test (SFT), to verify the fiber diameter estimations. Finally, the resulting permeability will be estimated using eq. (2) and (3) and the perspective for application in numerical simulations discussed.

2 METHODS

The characterization methods used in the present study are microscopy techniques and single fiber tests. All image analysis and post-processing of the characterization results were conducted in MATLAB. The characterization methods and the post-processing are described in the following subsections.

2.1 Microscopy

A small piece of the GF-PUR rod was embedded in an epoxy resin followed by standard grinding and polishing. The final polishing step applied was 1µm diamonds on a nap-cloth. LOM was carried out on a *Leica DMI 5000 Microscope* at ×10 magnification. The subsequent stitching of the LOM micrographs was conducted using the *PTGui Pro 11.8* software. The polished sample was then coated with carbon to make a conductive layer for the SEM to work with the non-conductive GF-PUR material. SEM imaging was conducted on a *Hitachi TM-1000 Tabletop Microscope* using an accelerating voltage of 15kV. The SEM micrographs were obtained at two magnifications; ×200 for fiber volume fraction characterization and ×1000 for fiber diameter characterization.

2.2 Single Fiber Test

Single glass fibers from textured yarns, similar to the fibers in the GF-PUR composite, were tested using a *Textechno Favimat+* single fiber test (SFT) setup. The glass fiber yarn was washed before the test to remove the sizing. The individual fibers, with a gauge length of 50mm, were put under pretension and then vibrated using a vibroscope. The eigenfrequency of the fiber was measured and the linear density subsequently obtained using the *Textechno* software. Finally, assuming a circular fiber cross-section and a density of 2.6g/cm³ the fiber diameter was readily obtained from the linear density.

2.3 Image Analysis and Post-Processing

The SEM micrographs at ×200 magnification were compared with the stitched LOM overview image and cropped to make a mosaic with no overlap (see Fig. 3). Subsequently, image analysis was conducted using simple binarization in MATLAB to obtain the fiber volume fraction. The cropped SEM images at ×200 magnification, see Fig. 3, were then all split into four new images in order to get a better resolution of the fiber volume fraction distribution. The SEM micrographs at ×1000 magnification was analysed using the *imfindcircles* built-in function in MATLAB to obtain the fiber center position as well as the fiber diameters.

A simple statistical analysis of calculating mean, standard deviations and making histograms was conducted for all the different data sets. Finally, assuming a hexagonal fiber packing [3], the fiber diameter and fiber volume fraction distribution results were used as input for permeability calculations, see eq. (2) and (3).

3 RESULTS AND DISCUSSION

Two micrographs from SEM at ×1000 magnification are shown in Fig. 1. The micrograph in Fig. 1 a) shows how porosities are located in-between highly agglomerated fibers. These porosities are only observed sporadically over the cross-section, but often in areas with high fiber volume fraction, hence the high fiber agglomeration (see Fig. 3).

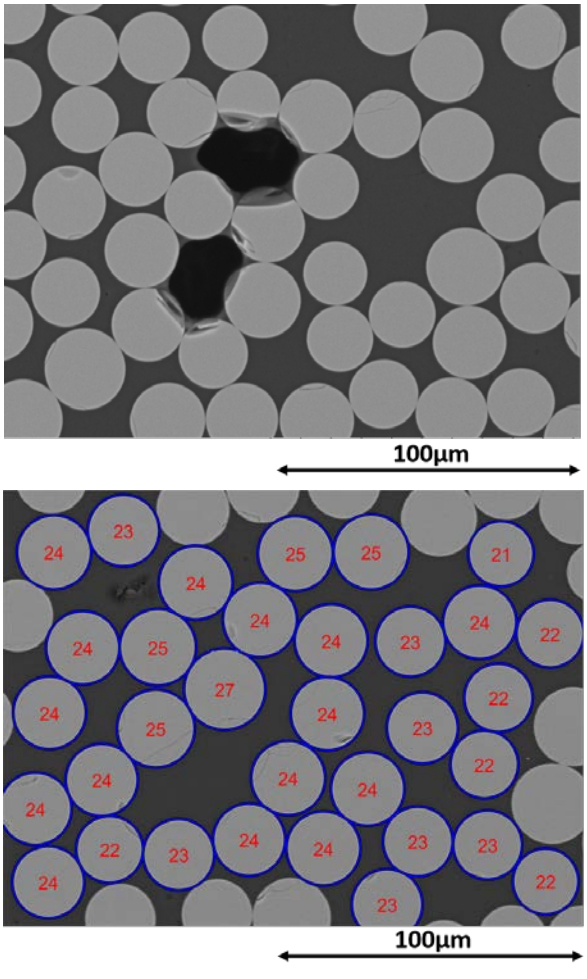

a)

b)

Figure 1: SEM micrographs at ×1000 magnification. a) SEM micrograph showing porosities in-between agglomerated fibers. b) Micrograph and overlaid fiber diameter analysis results in [µm].

The micrograph in Fig. 1 b) has the fiber diameter results plotted on top of the SEM image. It should be noticed how all full fibers in the image are detected while most fibers close to the edge are not detected. This problem was to some extend fixed by adjusting the input parameters for the *imfindcircles* function in MATLAB. Considering the objective of the current study, obtaining input for permeability estimations, the missing fiber detections would however not cause any significant deviations.

The fiber diameter distributions obtained from 20 SEM micrographs and 72 SFTs are depicted by histograms in Fig. 2. The 20 SEM micrographs covered two perpendicular diagonal lines of the Ø5mm cross-section. No significant fiber diameter distribution was observed as a function of cross-sectional position.

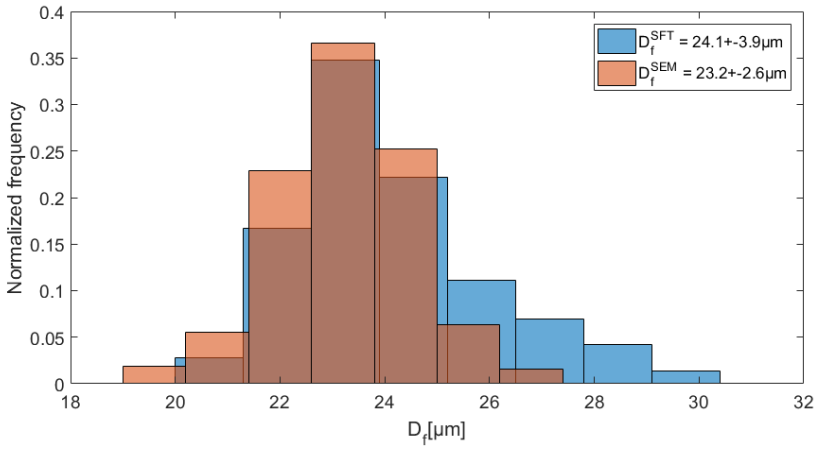

Figure 2: Fiber diameter distribution histogram and mean ± 2 standard deviations (legend) obtained from SEM micrographs and Single Fiber Tests (SFT).

From Fig. 2 it should be noticed how the fiber diameter distribution from SEM follows a normal distribution around a mean fiber diameter of approximately 23µm. It should further be noticed how the fiber diameter distribution obtained from SFTs is somewhat similar to the one obtained from the SEM micrographs, i.e. within the statistical uncertainty. However, the SFT seems to have a tendency of predicting a slightly larger fiber diameter. A possible source of error could be due to human error since more relative large diameter fibers might have been chosen do to ease of mounting.

The microscopy investigations, LOM and SEM (×200 magnification), was conducted to investigate the cross-sectional distribution of fiber volume fraction. A stitched overview-image of the full Ø5mm cross-section was obtained by LOM, see Fig. 3 a). A similar SEM overview mosaic image is shown in Fig. 3 b). Comparing Fig. 3 a) and b) it should be noticed how the manually cropped and binarized SEM images in the mosaic contain no cross-sectional areas twice but also do not miss any larger areas in the center part.

a) 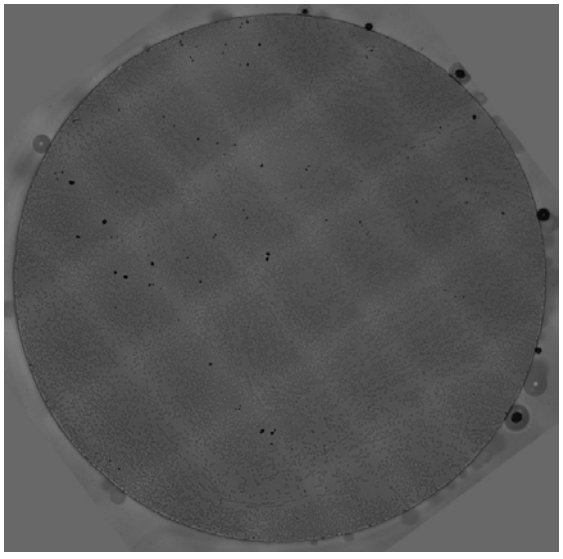

b) 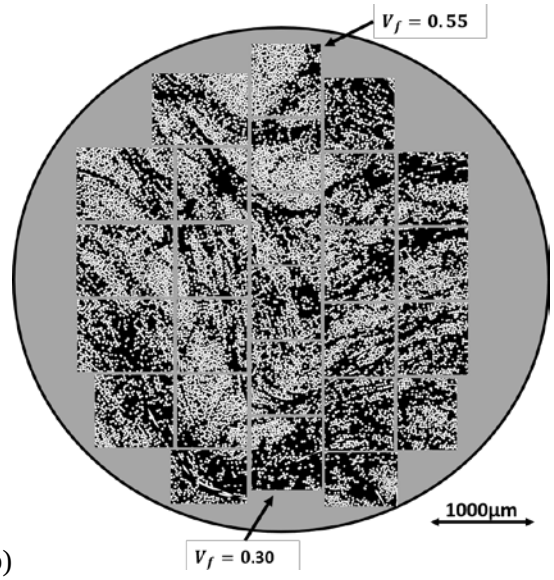

Figure 3: Cross-section of the Ø5mm GF-PUR rod:
a) Stitched micrographs from LOM. b) Binarized SEM micrograph mosaic.

The SEM images as depicted in Fig. 3 b) have a fiber volume fraction varying from 0.30 to 0.55 at the center column bottom and top micrograph, respectively. In order to illustrate the cross-sectional distribution of fiber volume fraction all the SEM images are assumed quadratic and extrapolations

were performed to obtain a rectangular grid to ease contour plotting. Fig. 4 a) illustrates the resulting contour plot of the cross-sectional fiber volume fraction. It should be noticed how Fig. 4 a) does not capture the high variance observed by the naked eye in Fig. 3 b). Hence, necessitating the subsequent image analysis described in subsection 2.3 - resulting in the refined contour plot depicted in Fig. 4 b).

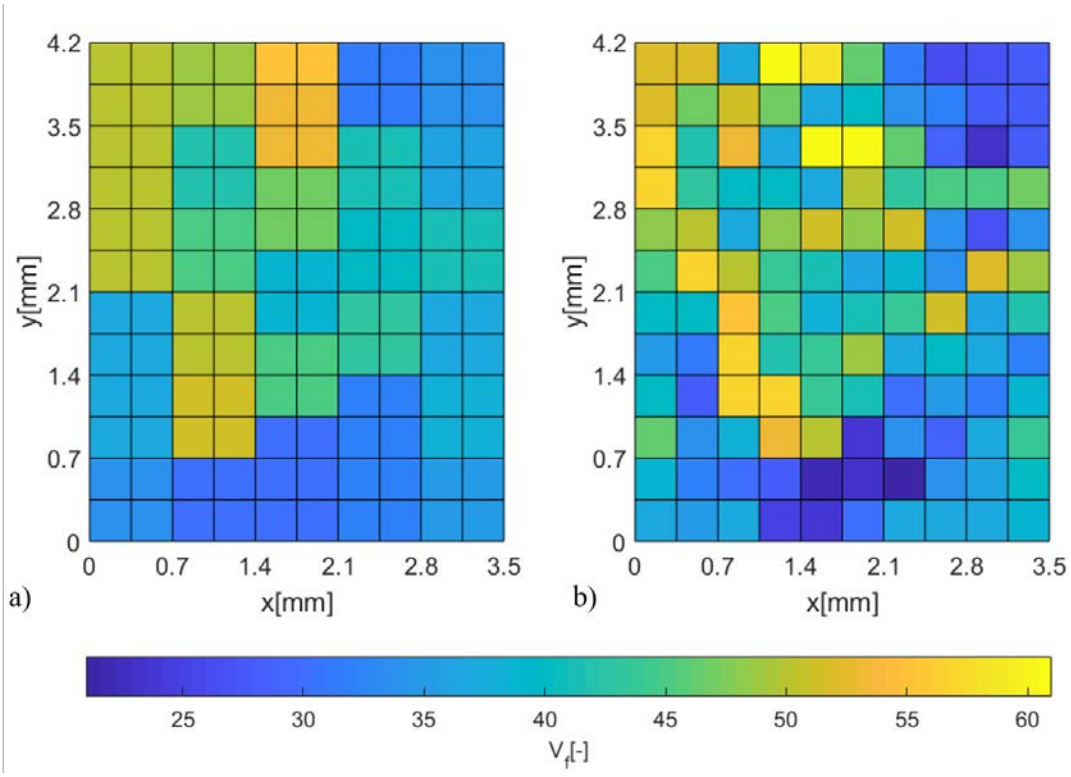

Figure 4: Distribution of fiber volume fraction: a) Original SEM image mesh. b) Refined mesh.

From Fig. 4 it should by noticed how the refined mesh (Fig. 4 b)) does a far better job of resolving the variance in fiber volume fraction distribution (see Fig. 3 b)) as compared with the original SEM image mesh (Fig. 4 a)). The same observation becomes very evident from a simple statistical analysis - depicted by histograms in Fig. 5.

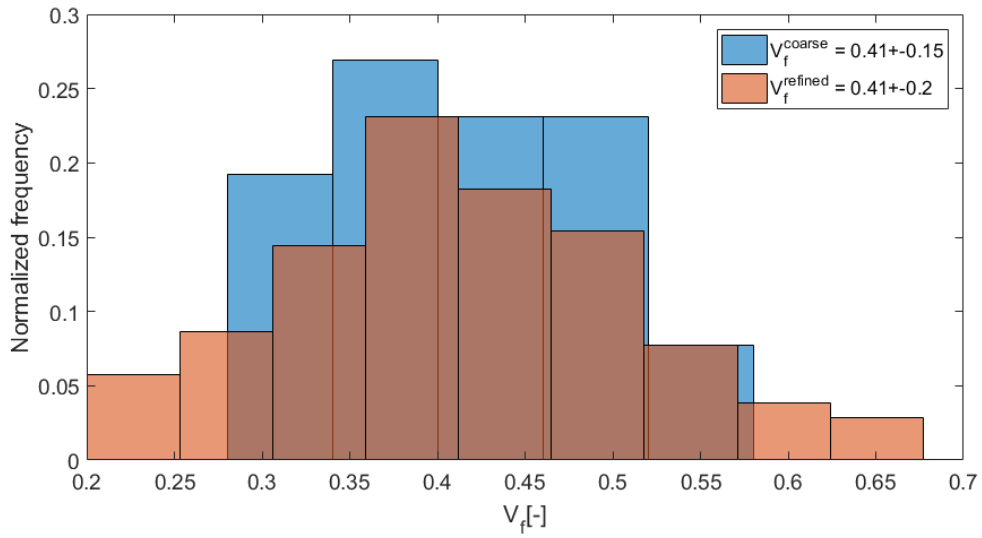

Figure 5: Fiber volume fraction distribution histograms and mean ± 2 standard deviations (legend) obtained from SEM micrographs – coarse vs refined mesh (see Fig. 4).

From Fig. 5 it should first of all be noticed that the mean fiber volume fraction, as expected, is independent of the mesh. However, the standard deviations, hence variance, does obviously depend on the mesh, i.e. number of observations. This only serves to support the fact that the refined mesh does a far better job of resolving the varying fiber volume fraction over the cross-section. Hence, only the refined mesh (Fig. 4 b)) will be considered for the permeability calculations.

Eq. (2) and (3) are used to calculate the transverse and axial permeability using a fiber diameter of 23.3µm and the varying fiber volume fraction as depicted in Fig. 4 b). The resulting transverse and axial permeability estimates over the cross-section are illustrated by contour plots in Fig. 6.

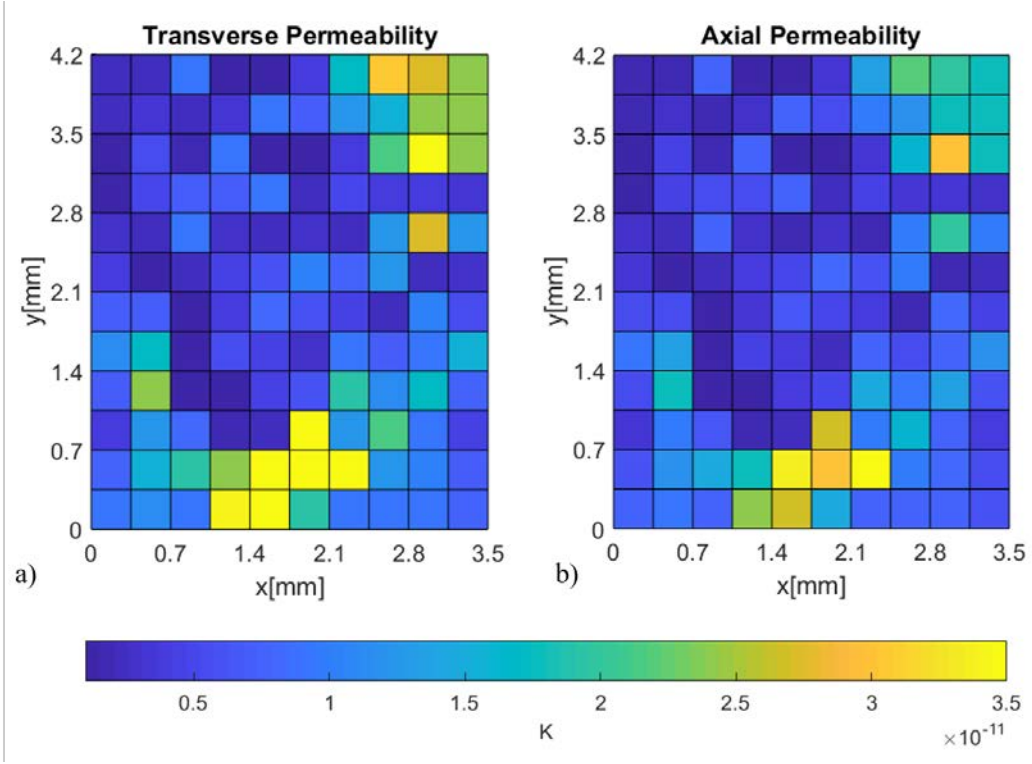

Figure 6: Permeability as a function of fiber volume fraction distribution (cf. Fig. 4 b)).
a) Transverse permeability. b) Axial permeability.

From a comparison of Fig. 6 and Fig. 4 b), it should in general be noticed how a high fiber volume fraction results in a lower permeability and vice versa. This is of course expected considering the fact that permeability is a measure of a material's ability to transmit fluids, but also considering the mathematical nature of eq. (2) and (3). The permeability results, as depicted in Fig. 6, illustrate a variance in the local cross-sectional permeability, with an axial and transverse permeability range of [3.4e-13 : 3.5e-11] and [4.0e-13 : 5.7e-11], respectively. The obtained permeability values are within the expected order of magnitude and show a high variance compared with results from literature [3,4]. Comparing Fig. 6 a) and b) it should be noticed how the transverse permeability scales more rapidly with changes in fiber volume fraction. This is why the range of the colour bar, in Fig. 6, is fixed with a max value of 3.5e-11. Hence, it is not possible to distinguish between permeability values above this max value – which is only the case for a few values of the transverse permeability in the lower middle region of the cross-section, see Fig. 6 a). The fixed range does however serve to pinpoint the abovementioned difference between the transverse and axial permeability (compare Fig. 6 a) and b)).

Considering manufacturing aspects of FRPs; numerical studies published by the authors have shown that a varying fiber volume fraction has a significant effect on the cure behaviour [7,8]. It seems obvious that a microstructure dependent permeability is an equally important input for impregnation simulations - ensuring good impregnation, low amounts of porosities and good mechanical properties. Hence, a fiber volume fraction dependent permeability, as depicted in Fig. 6, could serve as direct input for impregnation simulations governed by Darcy's Law.

4 CONCLUSION

The current study has investigated the cross-sectional variation in fiber volume fraction of a unidirectional glass fiber polyurethane rod as well as the resulting effect on local permeability. SEM images showed a very high contrast, resulting in high quality estimations of fiber diameter and fiber volume fraction. A mean fiber volume fraction of 0.41±0.2 and a mean fiber diameter of 23.2±2.6µm were obtained from the SEM investigations. The mean fiber volume fraction is in agreement with the fiber volume fraction of 0.41 obtained by burn-off test by the manufacturer. The fiber diameter estimates from SEM were compared with estimates from single fiber tests and found to be within the statistical uncertainty. The characterized fiber diameter and fiber volume fraction distribution were successfully applied for local permeability estimations resulting in an axial and transverse permeability range of [3.4e-13 : 3.5e-11] and [4.0e-13 : 5.7e-11], respectively. Hence, it is concluded that microstructure investigations by scanning electron microscopy can be used to obtain a microstructure dependent permeability directly applicable for numerical simulations.

ACKNOWLEDGEMENTS

This work is part of the *Resin Injection Pultrusion (RIP)* project which has been granted by the Danish Council for Independent Research | Technology and Production Sciences (DFF/FTP), Grant no. DFF-6111-00112.

I would like to acknowledge Senior Researcher, Søren Fæster (DTU Risø) for help with the SEM investigations.

REFERENCES

[1] O. Yuksel, I Baran, F. S. Rasmussen, J. Spangenberg, N. Ersoy, J. H. Hattel and R. Akkerman. Meso-scale process modelling strategies for pultrusion of unidirectional profiles. *Proceedings of the 18th European Conference on Composite Materials.* Athens Greece, 24-28th June 2018.

[2] P. C. Carman. Fluid flow through granular beds. *Trans. Int. Chem. Eng.*, 15:150-166, 1937.

[3] B. R. Gebart. Permeability of unidirectional reinforcements for RTM. *Journal of composite materials*. Vol. 26, No 8, 1992.

[4] G. Bechtold and L. Ye. Influence of fiber distribution on the transverse flow permeability in fiber bundles. *Composite science and technology*, 63:2069-2079, 2003.

[5] K. J. Ahn and J. C. Seferis. Simultaneous Measurements of permeability and capillary pressure of thermosetting matrices in woven fabric reinforcements. *Polymer composites*, Vol. 12, 3:146-152, June 1991.

[6] R. Bezerra, F. Wilhelm and F. Henning. Compressibility and permeability of fiber reinforcements for pultrusion. *Proceedings of the 16th European conference on composite materials.* Sevilla Spain, 22-26th June 2014.

[7] F. S. Rasmussen, C. G. Klingaa, M. Larsen, M. R. Sonne, J. Spangenberg and J. H. Hattel. Modelling the Effect of Non-Uniform Fiber Distribution on the Curing Behaviour in Resin Injection Pultrusion. *Proceedings of the 18th European Conference on Composite Materials.* Athens Greece, 24-28th June 2018.

[8] F. S. Rasmussen, C. G. Klingaa, M. R. Sonne and J. H. Hattel. *Numerical Modelling of Heat Transfer using the 3D-ADI-DG Method – with Application for Pultrusion*. 1st edition, Department of Mechanical Engineering, Technical University of Denmark, 2019.